Supplementary information

Tables

A) Kinetic matrix for fast decaying population of P^* (rate constants in 1/ps).

from/to	$\mathbf{P_F^*}$	$\mathbf{P^+B_L^-}$	$\mathbf{P^+H_L^-}$	$\mathbf{P^+Q_A^-}$	**GS**
$\mathbf{B_L^*/B_M^*}$	6.1	0	0	0	0
$\mathbf{P_F^*}$		0.056	0	0	0
$\mathbf{P^+B_L^-}$	0.056		0.1188	0	0
$\mathbf{P^+H_L^-}$	0	0.001188		0.003663	0
$\mathbf{P^+Q_A^-}$	0	0	0		$<10^{-4}$

Kinetic matrix for slowly decaying population of P^* (rate constants in 1/ps).

from/to	$\mathbf{P_S^*}$	$\mathbf{P^+B_L^-}$	$\mathbf{P^+H_L^-}$	$\mathbf{P^+Q_A^-}$	**GS**
$\mathbf{B_L^*/B_M^*}$	6.1	0	0	0	0
$\mathbf{P_S^*}$		0.018	0	0	0
$\mathbf{P^+B_L^-}$	0.018		0.1188	0	0
$\mathbf{P^+H_L^-}$	0	0.001188		0.003663	0
$\mathbf{P^+Q_A^-}$	0	0	0		$<10^{-4}$

B) Amplitude matrix for fast decaying population of P^* (72.8% of total).

Lifetime	$\mathbf{B_L^*/B_M^*}$	$\mathbf{P_F^*}$	$\mathbf{P^+B_L^-}$	$\mathbf{P^+H_L^-}$	$\mathbf{P^+Q_A^-}$
160 fs	**0.728**	**-0.735**	0.007	0	0
5.0 ps	0	0.102	**-0.258**	0.158	-0.003
29.0 ps	0	**0.624**	**0.242**	**-0.968**	0.103
279.0 ps	0	0.009	0.009	**0.810**	**-0.834**
long lived	0	0	0	0	**0.734**

Amplitude matrix for slowly decaying population of P^* (27.2% of total).

Lifetime	$\mathbf{B_L^*/B_M^*}$	$\mathbf{P_S^*}$	$\mathbf{P^+B_L^-}$	$\mathbf{P^+H_L^-}$	$\mathbf{P^+Q_A^-}$
160 fs	**0.272**	**-0.273**	0.001	0	0
7.1 ps	0	0.006	**-0.040**	0.035	-0.001
63.5 ps	0	**0.262**	**0.036**	**-0.387**	0.090
279.5 ps	0	0.005	0.004	**0.352**	**-0.363**
long lived	0	0	0	0	**0.274**

Supplementary Table 1 Kinetic matrix (A) and amplitude matrix (B) for the kinetic scheme shown in Fig. 5A. Values are from analysis of the data obtained with 805 nm excitation. Positive and negative amplitudes denote the decay and rise, respectively of the concentration of the corresponding compartment. Note that the sum of all amplitudes in a column corresponds to the amount of excitation. Numbers in bold indicate the most important decay terms for each species.

P^* modes	
1692(-)/1668(+)	9-keto C=O of P_LP_M/P^*
$P^+H_L^-$ modes	
P/P^+ modes	
1689(-)/1715(+)	9-keto C=O of P_L/P_L^+
1689(-)/1705(+)	9-keto C=O of P_M/P_M^+
1623(-)/1635(+)	2a-acetyl C=O of P_L/P_L^+
1639(-)/1643(+)	2a-acetyl C=O of P_M/P_M^+
1742(-)/1750(+)	10a-ester C=O of $P_LP_M/P_L^+P_M^+$
H_L/H_L^- modes	
1676(-)/1591(+	9-keto C=O of H_L/H_L^- hydrogen bonded to Glu L104
1728(-)/1736(+)	10a-ester C=O of H_L/H_L^-
protein modes	
1651(-)/1660(+)	up-shift of one or more amide I C=O in response to $P^+H_L^-$ formation
1651(-)/1643(+)	conformational changes in the protein backbone due to H_L^- formation and/or further H_L^- relaxation
$P^+Q_A^-$ modes	
P/P^+ modes	
1690(-)/1715(+)	9-keto C=O of P_L/P_L^+
1690(-)/1705(+)	9-keto C=O of P_M/P_M^+
1740(-)/1750(+)	10a-ester C=O of $P_LP_M/P_L^+P_M^+$
1726(-)/1730(+)	10a-ester C=O of H_L in electric field of Q_A/Q_A^-
Q_A/Q_A^- modes	
1631(-)/1612(+)	2a-acetyl C=O of Q_A/Q_A^- transition
1603(-)	2a-acetyl C=O of Q_A
protein modes	
1666(-)/1655(+)	protein amide I transition on Q_A/Q_A^-
1650(-)/1643(+)	response of a protein backbone C=O connected to Q_A via a H-bond perturbed upon Q_A^- formation
$P^+B_L^-$ modes	
P/P^+ modes	
1688(-)/1715(+)	9-keto C=O of P_L/P_L^+
1688(-)/1705(+)	9-keto C=O of P_M/P_M^+
1740(-)/1750(+)	10a-ester C=O of $P_LP_M/P_L^+P_M^+$
B_L/B_L^- modes	
1675-1680(-)	9-keto C=O of B_L
1663(+)	9-keto C=O of B_L^-
1612(+)	9-keto C=O of B_L^-
protein modes	
1651(-)/1643(+)	response of protein C=O group

Supplementary Table 2 Assignments of positive and negative bands observed in the SADS of the YM210W RC.

Figures

Supplementary Figure 1 Two representative time traces for YM210W RCs (squares) and R-26 RCs (circles) excited at 860 nm and probed at 1686 cm^{-1} or 1704 cm^{-1}. The solid lines through the data points are the result of a global fit using a sequential model. The time axis is linear up to 3 ps and logarithmic thereafter. The instrument response function was 150 fs fwhm.

Supplementary Figure 2 Time trace of YM210W RCs excited at 805 nm and probed at 1657 cm^{-1}. The solid lines through the data points are the result of fitting using model with two radical pairs (black line) or model consisting three radical pairs: model-III (red line).

Supplementary Figure 3 Comparison of SADS resulting from target analysis of the four data sets recorded for YM210W RCs. Key: solid spectra – 600 nm excitation, dashed spectra – 805 nm excitation, dotted spectra – 860 nm excitation and dash-dotted spectra – 795 nm excitation.

Supplementary Figure 4 Comparison of absorbance difference spectra measured at five selected delay times after excitation of YM210W RCs at 795, 805 and 860 nm.

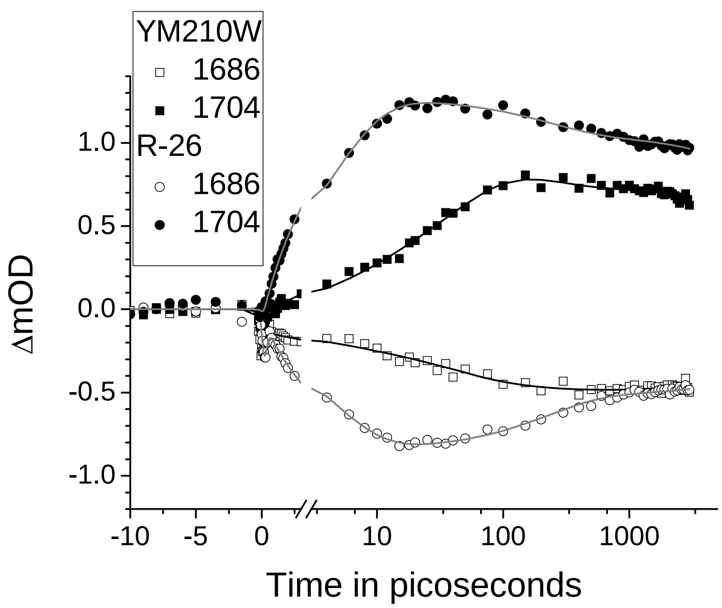

Supplementary Figure 1.

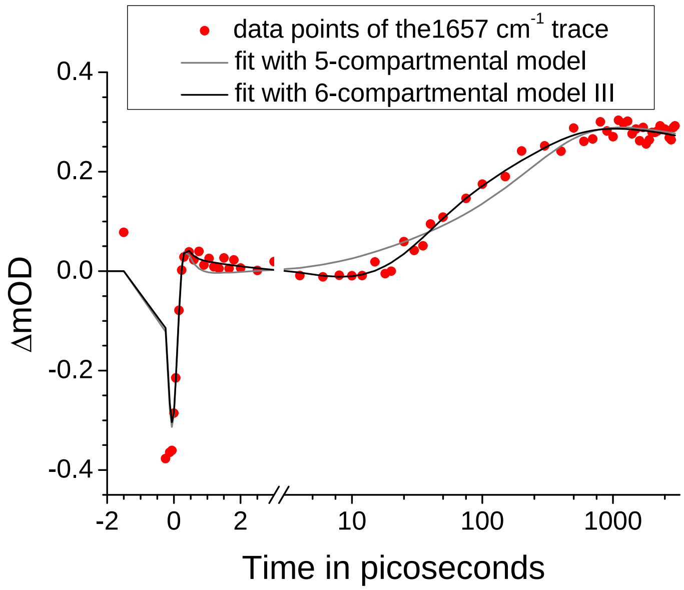

Supplementary Figure 2.

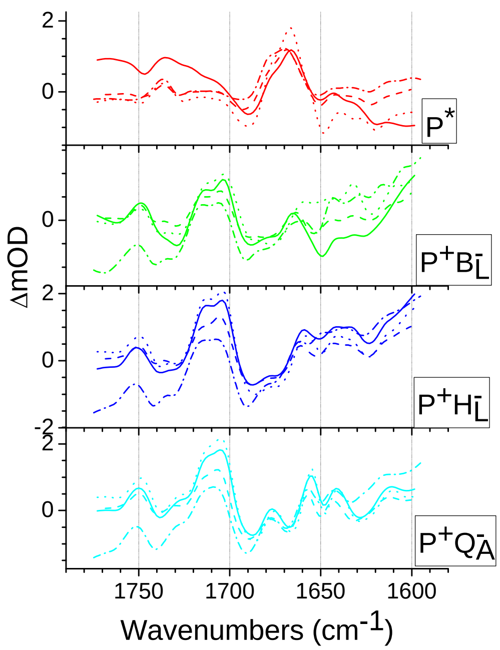

Supplementary Figure 3.

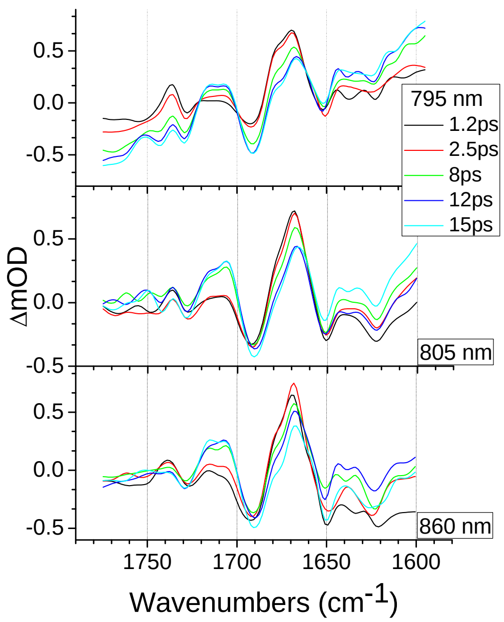

Supplementary Figure 4.